



Provided by the author(s) and University of Galway in accordance with publisher policies. Please cite the published version when available.

Title	A comparative reactivity study of 1-alkene fuels from ethylene to 1-heptene
Author(s)	Dong, Shijun; Zhang, Kuiwen; Senecal, Peter K.; Kukkadapu, Goutham; Wagnon, Scott W.; Barrett, Stephen; Lokachari, Nitin; Panigaphy, Snehasish; Pitz, William J.; Curran, Henry J.
Publication Date	2020-09-23
Publication Information	Dong, Shijun, Zhang, Kuiwen, Senecal, Peter K., Kukkadapu, Goutham, Wagnon, Scott W., Barrett, Stephen, Lokachari, Nitin, Panigaphy, Snehasish, Pitz, William J., Curran, Henry J. (2021). A comparative reactivity study of 1-alkene fuels from ethylene to 1-heptene. <i>Proceedings of the Combustion Institute</i> , 38(1), 611-619. doi: https://doi.org/10.1016/j.proci.2020.07.053
Publisher	Elsevier
Link to publisher's version	https://doi.org/10.1016/j.proci.2020.07.053
Item record	http://hdl.handle.net/10379/16946
DOI	http://dx.doi.org/10.1016/j.proci.2020.07.053

Downloaded 2024-04-29T03:48:55Z

Some rights reserved. For more information, please see the item record link above.



A comparative reactivity study of 1-alkene fuels from ethylene to 1-heptene

Shijun Dong^{a,*}, Kuiwen Zhang^{b,c}, Peter K. Senecal^c,
Goutham Kukkadapu^b, Scott W. Wagnon^b, Stephen Barrett^a,
Nitin Lokachari^a, Snehasish Panigaphy^a, William J. Pitz^b,
Henry J. Curran^a

^a Combustion Chemistry Centre, School of Chemistry, Ryan Institute, MaREI, NUI Galway, Ireland

^b Lawrence Livermore National Laboratory, Livermore, USA

^c Convergent Science, Madison, USA

Received 7 November 2019; accepted 2 July 2020

Available online 23 September 2020

Abstract

A comparative reactivity study of 1-alkene fuels from ethylene to 1-heptene has been performed using ignition delay time (IDT) measurements from both a high-pressure shock tube and a rapid compression machine, at an equivalence ratio of 1.0 in 'air', at a pressure of 30 atm in the temperature range of 600–1300 K. At low temperatures (< 950 K), the results show that 1-alkenes with longer carbon chains show higher fuel reactivity, with 1-pentene being the first fuel to show negative temperature coefficient (NTC) behavior followed by 1-hexene and 1-heptene. At high temperatures (> 950 K), the experimental results show that all of the fuels except propene show very similar fuel reactivity, with the IDTs of propene being approximately four times longer than for all of the other 1-alkenes. To analyze the experimental results, a chemistry mechanism has been developed using consistent rate constants for these alkenes. At 650 K, flux analyses show that hydroxyl radicals add to the double bond, followed by addition to molecular oxygen producing hydroxy-alkylperoxy radicals, which can proceed via the Waddington mechanism or alternate internal H-atom isomerizations in chain branching similar to those for alkanes. We have found that the major chain propagation reaction pathways that compete with chain branching pathways mainly produce hydroxyl rather than hydroperoxyl radicals, which explains the less pronounced NTC behavior for larger 1-alkenes compared to their corresponding alkanes. At 1200 K, flux analyses show that the accumulation of hydroperoxyl radicals is important for the auto-ignition of 1-alkenes from propene to 1-heptene. The rate of production of hydroperoxyl radicals for 1-alkenes from 1-butene to 1-heptene is higher than that for propene, which is due to the longer carbon chain

* Corresponding author.

E-mail address: shijun.dong@nuigalway.ie (S. Dong).

facilitating hydroperoxyl radical formation via more efficient reaction pathways. This is the major reason that propene presents lower fuel reactivity than the other 1-alkenes at high temperatures.

© 2020 The Authors. Published by Elsevier Inc. on behalf of The Combustion Institute.

This is an open access article under the CC BY license (<http://creativecommons.org/licenses/by/4.0/>)

Keywords: 1-Alkene; Ignition delay time; NTC; Chemistry mechanism

1. Introduction

Alkenes are important components in practical gasoline [1]. The higher research octane numbers of alkenes compared to their corresponding alkanes can directly affect auto-ignition behavior, and the unsaturated carbon bond can also contribute to soot formation [2]. Thus, it is important to understand alkene fuel chemistry. The fuel chemistry of alkenes has been extensively studied experimentally and theoretically over the years, and a significant number of kinetic models have been proposed [3]. Due to the presence of the C=C double bond, alkene chemistry can be considerably different to the corresponding alkane. Moreover, both the number and position of the C=C double bond can have a significant effect on fuel reactivity [8].

The linear 1-alkenes from ethylene to 1-heptene have similar structures but different carbon lengths, which indicate that they have some reaction pathways in common while the increased carbon length may facilitate difference reaction pathways. Therefore, a direct fuel reactivity comparison of these 1-alkenes can help us understand alkene fuel chemistry. Moreover, as alkenes are major products of the β -scissions of alkyl radicals [10], a direct comparison of alkene fuel reactivity can also help us understand alkane fuel reactivity at high temperatures. Unfortunately, most of the experimental data available in previous alkene studies are taken in different facilities, with mixtures at different degrees of dilution and at different conditions of pressure, temperature and equivalence ratio. Thus, it is difficult to directly compare the fuel reactivity of these alkenes.

Meanwhile, most alkene mechanisms have been proposed by different groups at different times [3,5,7] and the suggested important reaction pathways and rate constants used for the same reaction classes can be different. As a result, a detailed understanding of alkene chemistry is still not available. For instance, the reaction pathways controlling low-temperature chemistry remain unclear. In some papers it is suggested that it is due to alkenyl-peroxy radical chemistry while other papers suggested hydroxy-alkylperoxy radical reactions are the major factor [11]. Also, the reaction pathways of allyl-peroxy radicals are also not fully understood. Some studies show that allyl-peroxy radicals just decompose back to allylic

radicals and molecular oxygen [12], while other studies believe they can undergo further reactions and contribute to low-temperature chemistry [8]. Moreover, different branching ratios of hydroxyl radical addition to the terminal and central carbon sites of alkenes have been used [5,9]. Furthermore, alkenes are important intermediate species formed during the oxidation of alkanes. Some common reaction pathways can affect alkene, alkane and alcohol chemistry [13]. Thus, it is preferable to validate these mechanisms simultaneously [14]. Some quantum calculations have been published for alkene chemistry [15–17], which has aided our understanding of alkene chemistry.

Kikui et al. [18] compared the combustion and ignition characteristics of different 1-alkenes from ethylene to 1-pentene based on weak flame positions in a micro flow reactor. As the temperature of the micro flow reactor is not constant along the tube, the ignition is more like an integration result of different temperatures. Ribaucour et al. [6] studied the auto-ignition of 1-pentene in a rapid compression machine (RCM) at 700–900 K and $p = 7.5$ bar and observed a less pronounced NTC behavior compared to alkanes. 1-Butene was studied at higher pressures by Li et al. [5] who found that it does not show any NTC behavior. Thus, comparing directly the reactivity of 1-butene and 1-pentene at the same conditions and determining the reactions controlling their oxidation in the temperature range 600–900 K can help us understand the chemistry of NTC behavior for all 1-alkenes larger than C₄, as observed for 1-pentene, 1-hexene [8] and 1-heptene [19].

In this paper, ignition delay times (IDTs) of 1-alkenes from ethylene to 1-heptene over a wide temperature range (600–1300 K) at high pressure (30 atm) conditions have been measured using both a high-pressure shock tube (HPST) and an RCM. Moreover, a kinetic model, which captures the auto-ignition behavior of all of these 1-alkenes using consistent rate constants has been developed. Based on this model, flux analyses have been performed to understand the controlling chemistry.

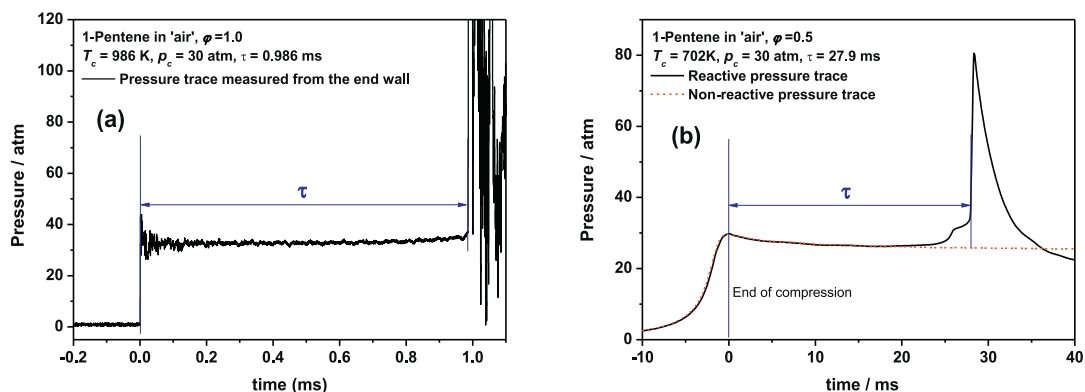


Fig. 1. Definition of ignition delay time measured in HPST (a) and RCM (b).

2. Experimental specifications

Detailed descriptions of the HPST and RCM facilities and the experimental procedures have been reported previously [20,21].

As discussed above, IDTs of ethylene, propene, 1-pentene, 1-hexene and 1-heptene have been measured for fuel/‘air’ mixtures at relatively high pressure (30 atm) and over a wide temperature range (600–1300 K). In the experiments, ‘air’ refers to the diluent (nitrogen or argon) and oxygen in the ratio 79:21. For the HPST experiments, only nitrogen was used as the diluent gas. For the RCM experiments, at some conditions 40% N_2 was replaced with Ar to achieve higher compressed gas temperatures. Moreover, for each test point a non-reactive pressure trace was recorded to simulate facility effects.

For the HPST experiments, the gas temperature and pressure behind the reflected shock wave were calculated using GasEq [22] based on the measured incident shock velocity and initial conditions of temperature, pressure and mixture composition. For the RCM experiments, the gas temperature after compression was calculated using GasEq based on the measured compressed pressure and initial conditions of pressure, temperature and mixture composition. The definitions of IDTs measured in both facilities are shown in Fig. 1. As discussed in previous studies [5], a 20% uncertainty is assigned to all of the IDT measurements.

High purity ethylene, propene, 1-pentene, 1-hexene and 1-heptene were provided by Sigma-Aldrich. The purity of all fuels is > 98.5%. High purity oxygen (> 99%), nitrogen (> 99%) and argon (> 99%) were provided by BOC.

3. Model development

The kinetic model is developed based the previous mechanisms published by NUI Galway and LLNL, ethylene [23], propene [3,4], 1-butene [5],

Table 1

Major updated reaction classes and references in the current model.

No.	Reaction pathways	Reference
1	$\dot{O}H$ addition on double bond	[27]
2	Waddington mechanism, Hydroxy-alkylperoxy radical isomerization and HO_2 elimination	[15]
3	Alkenyl-peroxy radical isomerization and decomposition	[12,16]
4	Alkene+ H_2O_2	[13]

the pentane isomers [10], *n*-hexane [24], hexene [25] and *n*-heptane [26]. The low- to intermediate-temperature chemistry of the propene, 1-butene, and 1-hexene mechanisms have been updated with consistent rate constants that were used for 1-pentene and 1-heptene model development. Table 1 shows a list of some important reaction classes updated and the corresponding references. Also, a new base model, NUIGMech1.0, was used in the development of the current model and the final mechanism is available as Supplementary material.

As allyl-peroxy radicals are thermochemically less stable than alkyl-peroxy radicals, the reverse rate constant is determined by the thermochemistry of O_2 and the relevant allyl and allyl-peroxy radicals and hence the degree of reactivity predicted by the resulting mechanism depends entirely on accurate thermochemistry. The thermochemistry of these allyl-hydroperoxides in the literature [16,28–30] was compared, including C_3H_5-3OOH , C_4H_7-3OOH , $trans-C_4H_7-1OOH$ etc., and a slight discrepancy between the entropy from these studies was observed (the species notation here is defined in a species dictionary included with the Supplemental material). In this study, the thermochemistry of C_4H_7-3OOH was estimated

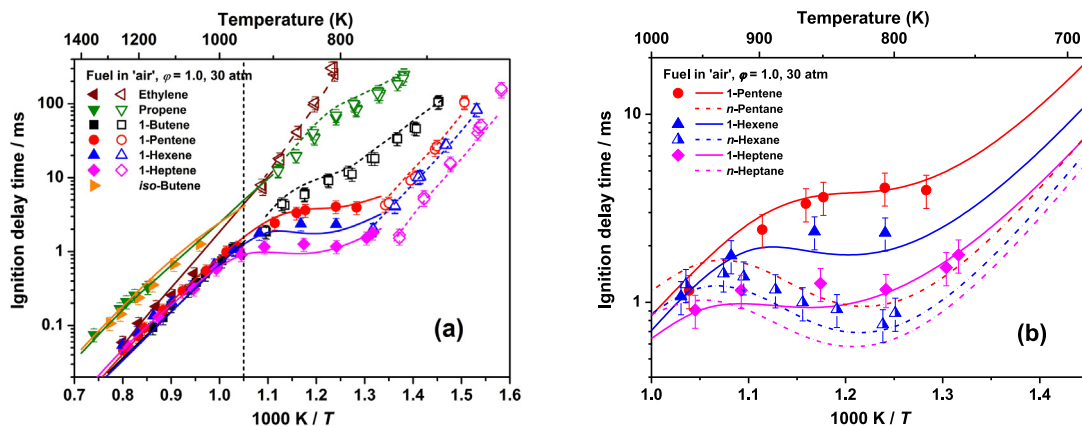


Fig. 2. (a) Experimental and simulated results of 1-alkenes from ethylene to 1-heptene. Solid symbols: HPST data. Open symbols: RCM data. Solid lines: constant-volume simulations. Dashed lines: RCM simulations including facility effect. 1-Butene data from [5] and isobutene data from [11]. (b) Comparison of NTC behavior between 1-alkenes and the corresponding alkanes. n-Hexane HPST data from [24] is measured at similar conditions. The dash-dotted lines represent simulated results using the mechanisms from [10] (nC₅), [24] (nC₆) and [26] (nC₇).

at the G3B3 level of theory and compared to values in the literature. These values have been used to update the group values used to generate the thermochemistry of allyl-hydroperoxides and their radicals using THERM [31]. In this study, the thermochemistry used is consistent for all radical species associated with the low-temperature kinetics of alkenes.

The simulations of IDTs measured in both the HPST and RCM were performed using Chemkin-Pro [32]. The HPST data are simulated assuming constant volume conditions. For the RCM simulations, effective volume history profiles derived from the non-reactive pressure traces were used to account for the facility effects in the RCM. Moreover, flux and sensitivity analyses were also performed using Chemkin-Pro.

4. Results and discussions

4.1. Model performance against experimental data

Figure 2(a) shows a comparison of the experimental and simulated results using the current model. As the uncertainty of the experimental data is about 20%, and all of the IDTs are measured over the same temperature ranges in the same facilities, a direct comparison of these results is reasonable, and the derived conclusions should be reliable. As for the HPST experiments for both ethylene and propene, there was a trend of pre-ignition when IDTs are approximately 1 ms, thus only experimental results for experiments without pre-ignition are included in Fig. 2(a). When the measured IDTs in RCMs are shorter than 5 ms the RCM data tend to deviate from the data measured in the HPST, which is due to the non-negligible chemical reac-

tion and heat release in the mixture during compression. It can be seen that the current model captures well the auto-ignition behavior of all of the 1-alkenes. For ethylene, the slope of the predictions is slightly different compared to the experimental results in the intermediate-temperature regime. At temperatures below 950 K we see that fuel reactivity increases with longer carbon chain lengths. Starting in molecular size from ethylene to 1-heptene, 1-pentene is the first fuel to show an NTC behavior, with 1-hexene and 1-heptene also showing similar NTC behavior with the fuels becoming progressively more reactive as they grow in carbon chain-length. Also, a comparison of the auto-ignition behavior in the NTC region between 1-alkenes and their corresponding alkanes is provided in Fig. 2(b). All of these large 1-alkenes are slower than their corresponding alkanes at temperatures below 900 K and they also show a less pronounced NTC behavior (i.e. the slope is not as steep), which indicate that the chemistry controlling the NTC behavior of alkenes differs somewhat compared to alkanes. At high temperatures (> 950 K), all 1-alkenes, except for propene, show almost identical reactivity, indicating that their reactivity may be controlled by the same chemistry. The IDTs of propene are approximately four times longer than for all other 1-alkenes. In Fig. 2(a) we have also included IDTs for isobutene at the same conditions, measured in the same facility [11]. Isobutene shows very similar reactivity to propene at high temperatures, indicating that the chemistry of these fuels is controlled by a different chemistry compared to the other 1-alkenes.

4.2. Flux analyses based on the current model

To further analyze the experimental results shown in Fig. 2, flux analyses for the 1-alkenes have been performed using the current model at different temperatures, Fig. 3. As 1-butene does not show NTC behavior and 1-pentene does, the low-temperature reaction pathways of 1-butene and 1-pentene are first compared to determine the reaction pathways that leading to NTC behavior of larger alkenes.

At 650 K in Fig. 3(d), more than 96% of 1-pentene is consumed by reacting with hydroxyl radicals. About 31% is consumed via H-atom abstraction by hydroxyl radicals, leading to the formation of three different pentenyl radicals, with 1-penten-3-yl (\dot{C}_5H_91-3) being the major radical formed (18.9%) as it is resonantly stabilized. Most 1-penten-3-yl radicals react with $\dot{H}O_2$ and ultimately produce $C_5H_9\dot{O}1-3/ C_5H_9\dot{O}2-1$ and $\dot{O}H$. The other two pentenyl radicals, 1-penten-4-yl (\dot{C}_5H_91-4) and 1-penten-5-yl (\dot{C}_5H_91-5) mainly add to O_2 to form alkenyl-peroxy radicals. $C_5H_91-4\dot{O}_2$ radicals mainly undergo $\dot{H}O_2$ elimination to produce $1,3-C_5H_8 + \dot{H}O_2$ as the C–H bond of the allylic site is weaker and five-membered transition state (TS) ring H-atom isomerizations are involved. $C_5H_91-5\dot{O}_2$ radicals mainly undergo isomerization to hydroperoxy-alkenyl radicals followed by a second addition to O_2 leading to chain branching, as this sequence involves six-membered TS ring isomerizations. Therefore, for the reaction pathways of pentenyl radicals, reactive hydroxyl radicals are consumed by H-atom abstraction reactions while fewer hydroxyl radicals or less reactive hydroperoxyl radicals are produced due to the presence of the double bond in 1-pentene relative to *n*-pentane, thus decreasing the reactivity of 1-pentene relative to *n*-pentane. Approximately 65% of 1-pentene molecules are consumed via hydroxyl radical addition to the double bond, leading to the formation of $\dot{C}_5H_{10}OH1-2$ and $\dot{C}_5H_{10}OH2-1$ radicals. These add to O_2 to produce $C_5H_{10}OH1-2\dot{O}_2$ and $C_5H_{10}OH2-1\dot{O}_2$ radicals and can subsequently react via the Waddington mechanism by intramolecular abstraction of the alkoxy H-atom with subsequent decomposition of the hydroperoxy-alkoxy radical. $C_5H_{10}OH1-2\dot{O}_2$ and $C_5H_{10}OH2-1\dot{O}_2$ radicals can also undergo internal H-atom re-arrangements of available H-atoms on other carbon sites to form alcoholic hydroperoxyl-alkyl radicals which can add to O_2 and proceed to chain branching. For 1-pentene, almost 17% of the fuel flux proceeds via this chain branching pathway. Therefore, for 1-pentene, the $C_5H_{10}OH1-2\dot{O}_2$ and $C_5H_{10}OH2-1\dot{O}_2$ radicals and $C_5H_91-5\dot{O}_2$ radical contribute to chain branching reaction pathways, with the $C_5H_{10}OH1-2\dot{O}_2$ radical contributing most.

The NTC behavior observed in alkanes is believed to be mainly due to the fate of alkyl-peroxy ($\dot{R}O_2$) and hydroperoxy-alkyl ($\dot{Q}OOH$) radicals. Flux analysis results of *n*-pentane are provided in Fig. S1 for comparison. If these radicals undergo propagation reactions such as molecular elimination, $\dot{R}O_2 = \text{olefin} + \dot{H}O_2$, or $\dot{Q}OOH = \text{cyclic ether} + \dot{O}H$ or $\text{olefin} + \dot{H}O_2$ or other β -scission products this results in reduced reactivity. If $\dot{Q}OOH$ radicals add to O_2 , they can proceed to chain branching and increase reactivity. Moreover, the β -scission of alkyl radicals is another chain propagation reaction class competing with chain branching as it produces an olefin and a smaller alkyl radical. This competition between branching and propagation is responsible for the NTC behavior of alkanes [10]. However, for 1-alkenes the reasons for NTC behavior are slightly different. Firstly, the fuel flux producing hydroxyalkyl radicals that can contribute to low-temperature chemistry decreases with increasing temperature. Fig. 3 shows that the proportion of fuel flux undergoing $\dot{O}H$ addition to the double bond decreases with increasing temperature, because of competition with abstraction by $\dot{O}H$ radicals. Therefore, the concentration of hydroxyalkyl radicals that can undergo chain branching reaction pathways decreases with increasing temperature, and this is the main chain branching pathway for 1-alkenes at low temperatures. Secondly, the major chain propagation reaction pathways competing with chain branching are the Waddington mechanism and 1-penten-3-yl radical reactions with $\dot{H}O_2$, Fig. 3. Although hydroxy-alkylperoxy radical concentrations decrease significantly with increasing temperature, the fuel flux leading to 1-penten-3-yl radicals increases and the fuel flux leading through the Waddington mechanism only slightly decreases while the fuel flux through chain branching significantly decreases. Meanwhile, both the Waddington mechanism and the reaction of 1-penten-3-yl radicals with $\dot{H}O_2$ produces reactive $\dot{O}H$ radicals rather than less reactive $\dot{H}O_2$ radicals which are produced from alkyl-peroxy radical elimination reactions or alkyl radicals produced from β -scission of alkyl radicals in alkanes. As the chain propagation reaction mainly produces reactive $\dot{O}H$ radicals rather than $\dot{H}O_2$ radicals, the competition of chain propagation and chain branching reaction pathways shows a relatively smaller effect on auto-ignition for alkenes compared to alkanes. Therefore, a less pronounced NTC behavior is observed for 1-alkenes from 1-pentene to 1-heptene, compared to their corresponding alkanes, Fig. 2.

For 1-butene the reaction pathways of 1-buten-3-yl (\dot{C}_4H_71-3) and 1-buten-4-yl (\dot{C}_4H_71-4) radicals are similar to those for pentenyl radicals. The fuel flux of hydroxyalkyl radicals is slightly higher than that for 1-pentene as less H-atom abstraction reactions compete with $\dot{O}H$ radical additions

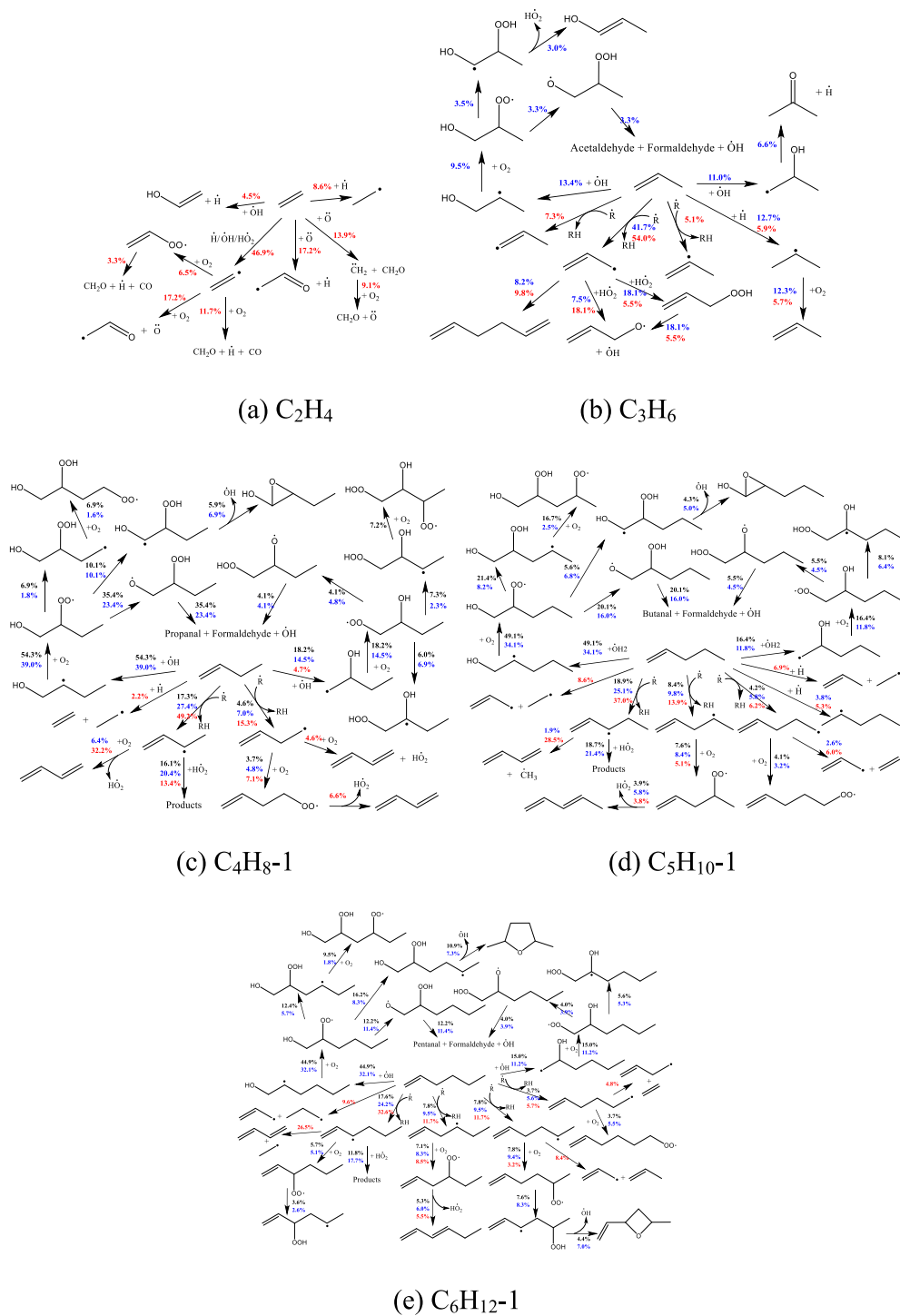


Fig. 3. Flux analyses for (a) ethylene, (b) propene, (c) 1-butene, (d) 1-pentene and (e) 1-hexene at $\varphi = 1.0$ in 'air', $p = 30$ atm and 20% fuel consumption. Numbers represent the percentage of fuel flux that goes into a particular species. Black numbers represent flux at 650 K, blue numbers represent flux at 800 K, and red numbers represent flux at 1200 K. \bar{R} is the sum of $\dot{O}H$, HO_2 and $\dot{C}H_3$ radicals and \dot{H} and \dot{O} atoms. Only reduced reaction pathways are given here and the detailed reaction pathways for all fuels are provided in Fig. S2.

across the double bond due to the shorter carbon chain. Following subsequent addition to O_2 , less fuel flux proceeds from $C_4H_8OH1-2O_2$ via a 1,5 H-shift leading to chain branching compared to $C_5H_{10}OH1-2O_2$, due to the stronger C–H bond of the primary carbon site as a 1,5 H-shift in $C_5H_{10}OH1-2O_2$ involves a secondary carbon site. Moreover, the 1,4 H-shift reaction competes with the 1,5 H-shift reaction due to the weaker C–H bond due to the presence of the hydroxyl group. This is the reason that 1-pentene shows NTC behavior while 1-butene does not. For 1-hexene, due to the longer carbon chain length, both 1-hexen-3-yl and 1-hexen-5-yl radicals can undergo chain branching reaction pathways and contribute to low-temperature fuel reactivity. This is the reason that 1-hexene shows a higher fuel reactivity compared to 1-pentene at low temperatures. Also, we see that the reaction pathways of alkenyl-peroxy radicals are important for linear 1-alkenes with carbon numbers larger than five.

At 1200 K, for all 1-alkenes most of the fuel is consumed by H-atom abstraction producing alkenyl radicals, with hydroxyalkyl reaction pathways no longer being important, Fig. 3. As propene shows a significantly lower fuel reactivity compared to ethylene and other larger 1-alkenes, its reaction pathways are compared to the others at high temperatures. Ethylene is the smallest fuel molecule studied but shows similar reactivity to the larger 1-alkenes, thus the reaction pathways of ethylene are first discussed. As shown in Fig. 3(a), almost 47% of ethylene is consumed by H-atom abstraction producing vinyl radicals and these can further produce \dot{H} and \dot{O} atoms and \dot{OH} radicals by reacting with O_2 at high temperatures, with the major chain branching reaction pathway being $\dot{C}_2H_3 + O_2 = \dot{C}H_2CHO + \dot{O}$. Moreover, more than 20% of the ethylene reacts with \dot{O} or \dot{OH} radicals producing \dot{H} atoms. These further react with O_2 in $\dot{H} + O_2 = \dot{O} + \dot{OH}$, which is the most important chain-branching reaction at high temperatures. This is the reason that ethylene shows relatively higher reactivity at high temperatures. However, due to the presence of the allylic site, only about 12% of propene is consumed via H-atom abstraction by \dot{HO}_2 radicals from the allylic site, which is chain branching as the H_2O_2 formed quickly decomposes to two \dot{OH} radicals at high temperatures. Alkyl radicals mostly react with \dot{HO}_2 and ultimately lead to the formation of allyloxy and hydroxyl radicals, competing with alkyl radical recombination which is chain terminating. However, there is no efficient reaction pathway for \dot{HO}_2 formation during the oxidation of propene. Thus, propene presents lower reactivity compared to ethylene. For larger 1-alkenes, the increased carbon chain facilitates

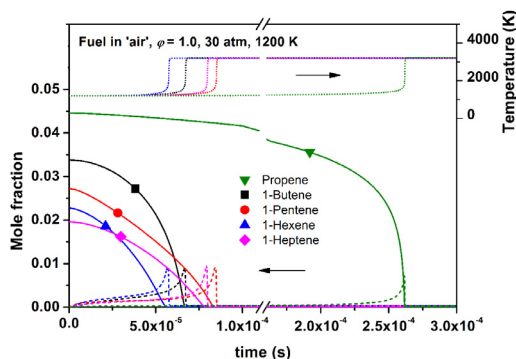


Fig. 4. Temperature and species mole fraction traces for different 1-alkenes. Short dot lines: temperature. Solid lines: fuel mole fraction. Dash lines: HO_2 mole fraction $\times 10$. Solid symbols: 20% fuel consumption timing.

more reaction pathways which promote fuel reactivity. The first is unimolecular decomposition which is chain branching. For 1-pentene, 1-hexene and 1-heptene, about 7% of the fuel is consumed via unimolecular decomposition, leading to the formation of allyl and alkyl radicals. For 1-butene, the flux through this reaction pathway is relatively small. The second pathway promoting reactivity is that leading to the formation of \dot{HO}_2 radicals. As discussed above, H-atom abstraction by \dot{HO}_2 radicals from the allylic site is chain branching, and allyl radicals are mostly consumed by reacting with \dot{HO}_2 radicals. As shown in Fig. 3, the reaction pathway of \dot{HO}_2 elimination from alkenyl-peroxy radicals is facilitated in 1-butene and larger 1-alkene oxidation. Moreover, the ethyl radicals produced during the oxidation of 1-butene and larger 1-alkenes mostly react with O_2 , leading to the formation of ethylene and \dot{HO}_2 radicals. However, there is no such efficient reaction pathway for \dot{HO}_2 formation during the oxidation of propene.

The mole fractions of \dot{HO}_2 radicals formed during the oxidation of these 1-alkenes are provided in Fig. 4. For 1-alkenes from propene to 1-heptene, auto-ignition occurs when the mole fractions of \dot{HO}_2 reach approximately 0.001. It takes considerably longer to form \dot{HO}_2 during propene oxidation. Thus, propene presents lower fuel reactivity than other larger 1-alkenes.

Almost 30% of the fuel flux for 1-butene, 1-pentene and 1-hexene leads to the formation of 1,3-butadiene, which is mainly consumed leading to the formation of vinyl radicals, as shown in Fig. S3. Moreover, significant quantities of ethylene and ethyl radicals are produced via direct decomposition of the fuel and β -scissions of alkenyl and/or alkyl radicals in the oxidation of the 1-olefins from 1-pentene to 1-heptene, and for 1-butene from β -scissions of radicals formed after \dot{H} , \dot{O} and \dot{OH}

additions to the double bond. Most ethyl radicals decompose to form ethylene. Thus, 1-butene and larger 1-alkenes share some reaction pathways similar to ethylene. This is the major reason that 1-butene and larger 1-alkenes show reactivity similar to ethylene.

5. Conclusions

- (1) At low temperatures (< 950 K), the experimental results show that the fuel reactivity of these 1-alkenes increase with the carbon chain length, and 1-pentene is the first fuel to show NTC behavior in the series from ethylene to 1-heptene.
- (2) At high temperatures (> 950 K), the experimental results show that all of the 1-alkenes except propene show very similar fuel reactivity, and propene shows significantly lower fuel reactivity than all of the other alkenes at this condition.
- (3) The current model can well capture the auto-ignition behavior of all of these 1-alkenes from low to high temperatures. The flux analyses performed at low temperatures show that reaction pathways of hydroxyalkyl radicals are the major reason for 1-alkene low-temperature chemistry. The less pronounced NTC behavior observed for larger 1-alkenes compared to the corresponding alkanes is mainly due to the following reason. The Waddington mechanism and the reaction of allyl radicals with HO_2 are the major competing channels with the chain branching reaction pathways, which mainly produce reactive $\dot{\text{O}}\text{H}$ rather than HO_2 radicals, which are produced by the major competing channel in alkanes. Therefore, the competition of chain branching with chain propagation has a relatively smaller effect on reactivity for alkenes compared to alkanes.
- (4) Flux analyses performed at high temperatures (~ 1200 K) show that the accumulation of HO_2 radicals is important for the auto-ignition of 1-alkenes from propene to 1-heptene, and the higher rate of production of HO_2 radicals for larger 1-alkenes (≥ 1 -butene) is responsible for the higher fuel reactivity of these compared to propene. 1-Butene and larger 1-alkenes share some reaction pathways similar to ethylene. This is the major reason that 1-butene and larger 1-alkenes show reactivity similar to ethylene.

Declaration of Competing Interest

None.

Acknowledgments

The authors at NUI Galway recognize funding support from Science Foundation Ireland (SFI) via their Research Centre Program through project number 16/SP/3829 and also funding from Computational Chemistry LLC. The work at LLNL was performed under the auspices of the U.S. Department of Energy (DOE) by Lawrence Livermore National Laboratory under Contract DE-AC52-07NA27344 and was conducted as part of the Co-Optimization of Fuels & Engines (Co-Optima) project sponsored by the DOE Office of Energy Efficiency and Renewable Energy (EERE), Bioenergy Technologies and Vehicle Technologies Offices.

Supplementary materials

Supplementary material associated with this article can be found, in the online version, at doi:10.1016/j.proci.2020.07.053.

References

- [1] C.V. Naik, W.J. Pitz, M. Sjöberg, et al. Detailed Chemical Kinetic Modelling of Surrogate Fuels for Gasoline and Application to an HCCI Engine, SAE Tech Paper 2005-01-3741, 2005.
- [2] S.M. Sarathy, A. Farooq, G.T. Kalghatgi, *Prog. Energy Combust. Sci.* 65 (2018) 67–108.
- [3] S.M. Burke, W. Metcalfe, O. Herbinet, et al., *Combust. Flame* 161 (2014) 2765–2784.
- [4] S.M. Burke, U. Burke, R. Mc Donagh, et al., *Combust. Flame* 162 (2015) 296–314.
- [5] Y. Li, C.W. Zhou, H.J. Curran, *Combust. Flame* 181 (2017) 198–213.
- [6] M. Ribaucour, R. Minetti, L.R. Sochet, in: *Proceedings of the Twenty-Seventh Symposium of Combustion Institute*, 1998, pp. 345–351.
- [7] S. Touchard, F. Buda, G. Dayma, P.A. Glaude, R. Fournet, F. Battin-Leclerc, *Int. J. Chem. Kinet.* 37 (2005) 451–463.
- [8] M. Mehl, G. Vanhove, W.J. Pitz, E. Ranzi, *Combust. Flame* 155 (2008) 756–772.
- [9] X. Meng, A. Rodriguez, O. Herbinet, T. Wang, F. Battin-Leclerc, *Combust. Flame* 181 (2017) 283–299.
- [10] J. Bugler, B. Marks, O. Mathieu, et al., *Combust. Flame* 163 (2016) 138–156.
- [11] C.W. Zhou, Y. Li, E. O'Connor, et al., *Combust. Flame* 167 (2016) 353–379.
- [12] X. You, Y. Chi, T. He, *J. Phys. Chem. A* 120 (2016) 5969–5978.
- [13] J. Zádor, S.J. Klippenstein, J.A. Miller, *J. Phys. Chem. A* 115 (2011) 10218–10225.
- [14] H.J. Curran, *Proc. Combust. Inst.* 37 (1) (2019) 57–81.
- [15] J.C. Lizardo-Huerta, B. Sirjean, R. Bounaceur, R. Fournet, *Phys. Chem. Chem. Phys.* 18 (2016) 12231–12251.
- [16] X. Sun, W. Zong, J. Wang, Z. Li, X. Li, *Phys. Chem. Chem. Phys.* 21 (2019) 10693–10705.
- [17] J. Zádor, A.W. Jasper, J.A. Miller, *Phys. Chem. Chem. Phys.* 11 (2009) 11040–11053.

- [18] S. Kikui, H. Nakamura, T. Tezuka, S. Hasegawa, K. Maruta, *Combust. Flame* 163 (2016) 209–219.
- [19] Y. Wu, Y. Liu, C. Tang, Z. Huang, *Combust. Flame* 197 (2018) 30–40.
- [20] D. Darcy, C.J. Tobin, K. Yasunaga, et al., *Combust. Flame* 159 (2012) 2219–2232.
- [21] D. Darcy, H. Nakamura, C.J. Tobin, et al., *Combust. Flame* 161 (2014) 65–74.
- [22] C. Morley, GasEq, Version 0.76. <http://www.gaseq.co.uk>, 2004.
- [23] C.W. Zhou, Y. Li, U. Burke, et al., *Combust. Flame* 197 (2018) 423–438.
- [24] K. Zhang, C. Banyon, C. Togbé, P. Dagaut, J. Bugler, H.J. Curran, *Combust. Flame* 162 (2015) 4194–4207.
- [25] G. Kukkadapu, K. Kumar, C.J. Sung, M. Mehl, W.J. Pitz, *Proc. Combust. Inst.* 34 (2013) 345–352.
- [26] K. Zhang, C. Banyon, J. Bugler, et al., *Combust. Flame* 172 (2016) 116–135.
- [27] I.O. Antonov, J. Kwok, J. Zádor, L. Sheps, *Phys. Chem. A* 119 (2015) 7742–7752.
- [28] J. Lee, J.W. Bozzelli, *Proc. Combust. Inst.* 30 (2005) 1015–1022.
- [29] M. Keçeli, S.N. Elliott, Y.P. Li, et al., *Proc. Combust. Inst.* 37 (2019) 363–371.
- [30] C.F. Goldsmith, G.R. Magoon, W.H. Green, *J. Phys. Chem. A* 116 (2012) 9033–9047.
- [31] E.R. Ritter, J.W. Bozzelli, *J. Chem. Kinet.* 23 (1991) 767–778.
- [32] CHEMKIN-PRO 15101, Reaction Design, San Diego, 2010.